Title (14 words)

RANKL regulates the differentiation of microfold cells in mouse nasopharynx-associated lymphoid tissue (NALT)

Authors

Mami Mutoh[1], Shunsuke Kimura[2], Hiromi Takahashi-Iwanaga[2], Meri Hisamoto[3], Toshihiko Iwanaga[2], and Junichiro Iida[1]

Affiliations

[1]Department of Orthodontics, Hokkaido University Graduate School of Dental Medicine, Sapporo 060-8586, Japan

[2]Laboratory of Histology and Cytology, Hokkaido University Graduate School of Medicine, Sapporo 060-8638, Japan

[3]Division of Oral Functional Prosthodontics, Department of Oral Pathobiological Science, Hokkaido University Graduate School of Dental Medicine, Sapporo, 060-8586, Japan

Abbreviations

GP2, Glycoprotein 2; NALT, Nasopharynx-associated lymphoid tissue; RANKL, Receptor activator of NFκB ligand; FAE, Follicle-associated epithelium

Correspondence

Shunsuke Kimura, Ph.D.

Address: North 15, West 7, Kita-ku, Sapporo 060-8638, Japan

Phone and FAX: +81-11-706-7151

E-mail address: skimu@med.hokudai.ac.jp

Disclosures

The authors disclose no conflicts of interests.

Acknowledgments

This study was supported by Grants-in-Aid for Scientific Research 25460261 (to S.K.).

Abstract (243/250 words)

Murine nasopharynx-associated lymphoid tissue (NALT), located at the base of the nasal cavity, serves as a predominant site for the induction of mucosal immune responses against airway antigens. The follicle-associated epithelium (FAE) covering the luminal surface of NALT is characterized by the presence of microfold cells (M cells), which take up and transport luminal antigens to lymphocytes. Glycoprotein 2 (GP2) was recently identified a reliable marker for M cells in Peyer's patches of the intestine. However, the expression of GP2 and other functional molecules in the M cells of NALT has not yet been examined. In the present study, we immunohistochemically detected GP2-expressing cells in the FAE of NALT and the simultaneous expression of other intestinal M-cell markers, Tnfaip2, CCL9, and Spi-B. These cells were functionally identified as M cells due to their uptake capacity of luminal microbeads. Electron microscopic observations showed that GP2-expressing cells on the FAE displayed morphological features typical of M cells; they possessed short microvilli and microfolds on the luminal surface and were closely associated with intraepithelial lymphocytes. We also found that the receptor activator of nuclear factor kappa-B ligand (RANKL) was expressed by stromal cells underneath the FAE, which provided its receptor RANK. Thus, the administration of RANKL markedly increased the number of $GP2^{+}Tnfaip2^{+}$ cells on the NALT FAE as well as that of intestinal M cells. These results suggest that $GP2^{+}Tnfaip2^{+}$ cells in NALT are equivalent to intestinal M cells, and RANKL-RANK signaling induces their differentiation.

Introduction

The mucosal surface of the nasopharyngeal cavity is exposed to a vast array of foreign antigens and microorganisms from inhaled air and ingested food. The nasal cavity in the rodent develops mucosal lymphoid tissues, collectively called nasopharynx (or nasal)-associated lymphoid tissue (NALT). NALT is nestled along both sides of the nasopharyngeal duct and is generally considered to correspond to Waldeyer's ring in humans (Kuper et al. 1990, 1992). Similar to Peyer's patches in the intestinal immune system, NALT may serve as an inductive site for mucosal immunity in the upper respiratory tract. NALT consists of follicle-associated epithelia (FAE), high endothelial venules, germinal centers, and T cell- and B cell-enriched areas (Brandtzaeg 1996; Stanley et al. 2001). NALT is a non-encapsulated mucosal lymphoid organ that does not possess afferent lymphatics, similar to Peyer's patches. The FAE of both tissues instead transports antigens from the lumen of the aerodigestive tracts to the underlying lymphoid tissues.

The M cell, the name of which is derived from "microfold" or "membranous" cell, is an epithelial cell type specialized for the uptake of macromolecules and is dispersed in the FAE of mucosa-associated lymphoid tissues, including NALT and gut-associated lymphoid tissues (GALT) (Mabbott et al. 2013). The morphology, topographical proximity to intraepithelial lymphocytes, and ability of M cells of NALT to take up luminal antigens are similar to those of intestinal M cells (Gebert et al. 1999). Histochemically, the M cells of NALT have been identified by the expression of cytokeratin 8, 18, 20, and vimentin in the rabbit palatine tonsil (Carapelli et al. 2004; Gebert et al. 1995; Jepson et al. 1992); the expression of clusterin and class II β-tubulin in the human Waldeyer's ring (Lee et al. 2010; Verbrugghe et al. 2008); and

affinity to *Ulex europaeus* agglutinin I (UEA-I) lectin in murine and rat NALT (Jeong et al. 1999; Kim et al. 2011). Recent studies identified various unique molecules expressed in the M cells of Peyer's patches. Among them, glycoprotein 2 (GP2) was recognized as a reliable indicator for mature and functional M cells in the intestine (Kimura et al. 2015). GP2 is expressed on the luminal surface of M cells and acts as a receptor that mediates the uptake of type-I-piliated bacteria residing in the gut (Hase et al. 2009a). Tnfaip2 is a cytosolic protein that is expressed in mature and immature M cells (Kimura et al. 2015) and is considered to play a role in intercellular communication among M cells (Hase et al. 2009b). However, the expression of GP2 and Tnfaip2 in NALT has not yet been examined.

The molecular basis of M-cell differentiation has been partially elucidated for intestinal M cells. The receptor activator of nuclear factor-κB (RANK) and its ligand (RANKL) are indispensable for initiating M-cell differentiation from Lgr5-positive epithelial stem cells (de Lau et al. 2012; Knoop et al. 2009). RelB and Spi-B, downstream transcription factors of RANKL-RANK signaling, were previously shown to be essential for the subsequent differentiation process toward the maturation of intestinal M cells (Kimura et al. 2015; Sato et al. 2013; de Lau et al. 2012; Kanaya et al. 2012). On the other hand, information regarding the factors required for M-cell differentiation in NALT is limited. Therefore, we herein investigated the expression profiles of M cell-related molecules in the NALT of mice. We also succeeded, for the first time, in inducing M cells in the ciliated epithelium of NALT using RANKL-RANK signaling.

Materials and methods

Mice

Seven- to 12-week-old BALB/cCrSlc (BALB/c) mice were purchased from Japan SLC (Hamamatsu, Japan), and maintained under conventional conditions. All experiments using animals were performed under protocols following the Guidelines for Animal Experimentation, of Hokkaido University Graduate School of Medicine.

Immunohistochemistry

Deeply anesthetized mice were perfused via the aorta with physiological saline followed by 4% paraformaldehyde (PFA), pH 7.4. The heads were removed and immersed in the same fixative for an additional 24 h, and then decalcified with 5% EDTA for 2 weeks at 4˚C. The decalcified tissues were dipped in 30% sucrose solution overnight at 4˚C, embedded in OCT compound (Sakura Finetek, Tokyo, Japan), and quickly frozen in liquid nitrogen. Frozen sections, approximately 14-μm thick, were mounted on gelatin-coated glass slides. After a pretreatment with 0.3% Triton X-100-containing PBS (pH 7.2) for 30 min and preincubation with 10% normal donkey serum, the sections were incubated with a rat anti-GP2 monoclonal antibody (1:200 dilution; MBL, Nagano, Japan) mixed with either rabbit anti-Tnfaip2 antibodies (1:200) (Kimura et al. 2015), goat anti-CCL9 antibodies (1:100; R&D systems, Minneapolis, MN), rabbit anti-RelB antibodies (1:200; Santa Cruz Biotechnology, Santa Cruz, CA), or UEA-I lectin (1:400; Vector Laboratories, Burlingame, CA) overnight. The sites of the antigen-antibody reaction were detected by an incubation with Cy5-labeled anti-rat IgG (1:400) mixed with Cy3-labeled anti-rabbit IgG (1:400) or Cy3-labeled anti-goat IgG antibodies (1:400)

obtained from Life Technologies (Paisley, U.K.).

To achieve Spi-B staining, sections were dipped in 0.1% H_2O_2 after the pretreatment with Triton X-100 and donkey serum in order to inhibit endogenous peroxidase activities. The sections were then incubated with sheep anti-Spi-B antibodies (1:200; R&D systems) overnight. The sites of the antigen-antibody reaction were detected by an incubation with horseradish peroxidase (HRP)-labeled anti-sheep IgG for 2 h. Tyramide signal amplification (TSA) plus amplification reagent were applied to the slides in accordance with the manufacturer's protocol (Perkin Elmer, Wellesley, MA)

Regarding triple immunofluorescence staining for RANKL, RANK, and Tnfaip2, mice were sacrificed by cervical dislocation. NALTs were separated from the upper jaw by peeling away the palate, as described previously (Asanuma et al. 1997). Fresh specimens were immediately embedded in OCT compound. Frozen sections were mounted on gelatin-coated glass slides, and fixed with ice-cold methanol at −20˚C for 10 min. The fixed sections were incubated with 10% normal donkey serum for 30 min at room temperature, and then treated with a primary antibody cocktail: a rat anti-RANKL monoclonal antibody (1:200 dilution; eBioscience, San Diego, CA, USA), goat anti-RANK antibodies (1:200), and rabbit anti-Tnfaip2 antibodies (1:200). After an overnight incubation, the sections were washed with PBS three times, and then incubated with secondary antibodies: a cocktail of Alexa488 anti-rat-IgG (1:400), Cy5 anti-goat IgG (1:400), and Cy3 anti-rabbit (1:400).

Fluorescent* in situ *hybridization (FISH)

FISH was performed using the Quantigene View RNA ISH Cell Assay (Affymetrix, Santa Clara,

CA, USA) with slight modifications in the fixation and protease digestion steps. Briefly, perfusion fixation was performed with a solution containing 4% PFA and 0.5% glutaraldehyde in PBS. The heads were removed and immersed in 4% PFA for an additional 24 h. The preparation of frozen sections was described as above. Sections were floated in 50 mM glycine in PBS and washed three times. The floating sections were pretreated with a detergent solution for 10 min and then protease QS (dilution 1:400 in PBS; Affymetrix) or 0.1 mg/ml proteinase K in PBS (Kanto Chemical co, Tokyo, Japan) for 10 min at room temperature. These processes were performed in accordance with the manufacturer's protocol. Specific oligonucleotide probe sets against *Gp2* (catalog No, VB6-13947), *Tnfaip2* (VB4-13531), and *Spib* (VB1-13735) were purchased from Affymetrix, Inc.

Silver-intensified immunogold method for transmission electron microscopy

PFA-fixed and decalcified tissues were dipped in 30% sucrose solution overnight at 4˚C, embedded in OCT compound, and quickly frozen in liquid nitrogen. Fifteen-micrometer-thick frozen sections were mounted on poly-L-lysine coated glass slides, incubated with the rat anti-GP2 antibody (1 μg/ml) overnight, and subsequently reacted with goat anti-rat IgG covalently linked with 1 nm gold particles (1:200 dilution; Nanoprobes, Yaphank, NY). Following silver enhancement with a kit (HQ silver; Nanoprobes), the sections were osmicated, dehydrated, and directly embedded in Epon (Nisshin EM, Tokyo, Japan). Ultrathin sections were prepared and stained with uranyl acetate and lead citrate for observations under an electron microscope (H-7100; Hitachi, Tokyo, Japan).

Scanning electron microscope observations of NALT

Two adult male mice (C57BL/6J, 24 g body weight, approximately 10 weeks old) were used. Under deep anesthesia by an intraperitoneal injection of sodium pentobarbital (60 mg/kg body weight), the nasal cavities of the animals were cannulated with fine polyethylene tubing through the right naris and then irrigated with 5 ml of saline. During nasal irrigation, the animals were perfused transcardially with 2.5% glutaraldehyde buffered at pH 7.4 with 0.1 M phosphate buffer. Following fixation, the upper jaws, including the nasal mucosa, were removed *en bloc* and immersed in the same fixative at 4˚C for an additional 12 h. The tissue blocks were decalcified with 5% EDTA-2Na, pH 7.4, for approximately 7 days at 4˚C. After decalcification, the lower posterior portion of the nasal cavity was removed with a razor blade, postfixed in 1% OsO_4 for 2 h, and conductive-stained with 1% tannic acid, followed by 1% OsO_4. Osmicated specimens were dehydrated with ethanol and critical-point-dried with liquid CO_2. The dried specimens were coated with osmium in a plasma osmium coater (Nippon Laser and Electronics Laboratory, Nagoya, Japan) and examined under a Hitachi SU8010 scanning electron microscope.

Nasal administration of latex beads

Aliquots of 1×10^{11} fluorescent polystyrene latex beads (20 nm in diameter; Life Technologies) were dropped into the nasal cavity of BALB/c mice three times. After a 30-min incubation, mice were sacrificed and subjected to immunohistochemical experiments.

RANKL administration

The purification of GST-RANKL and GST was described previously (Kimura et al. 2015). Purified protein was administered to mice by intraperitoneal injections of 250 μg per day for three days. Mice were sacrificed 24 h after the last administration and subjected to assays.

Results

Morphological characteristics of GP2-immunoreactive cells in NALT

A histological examination of frontal sections from decalcified mouse heads revealed that NALT was situated in the mucosa of both lateral walls at the nasal floor (Fig. 1a). Scanning electron microscopy showed that the M cells of NALT extended their characteristic stubby microvilli, which were approximately 300-nm thick, and short irregular microfolds from the luminal surface (Supplemental Fig. 1). In contrast, the surrounding cells were covered with long cilia and fine microvilli, with the latter being approximately 100-nm thickness. No cilia were detected on the surfaces of the M cells.

GP2 and Tnfaip2 are well-defined molecular markers for M cells in intestinal Peyer's patches (Hase et al. 2009a, 2009b; Kimura et al. 2015). We first stained NALT for the two molecules. Immunohistochemical experiments using the anti-GP2 monoclonal antibody displayed distinctive positive staining on epithelial cells that were scattered in the FAE. GP2-immunoreactive cells also reacted with the anti-Tnfaip2 antibody, the antigen of which was previously shown to be selectively expressed in intestinal M cells (Fig. 1b) (Hase et al. 2009b; Kimura et al. 2015). At a higher magnification, Tnfaip2 was found to be localized in the cytoplasm of cells, while GP2 signals occurred in the apical portion of cells and as puncta in the deeper region of the FAE (Fig. 1c and d).

Transmission electron microscopy showed that GP2-immunoreactive cells in the FAE of NALT lacked cilia on their apical surface and were closely associated with intraepithelial lymphocytes, which had an electron-lucent cytoplasm (Fig. 2a). Immunogold particles, showing the existence of GP2, accumulated on the apical plasma membrane undulated

stubby microvilli (Fig. 2b) and were denser along the lateral surface, which contacted intraepithelial lymphocytes (Fig. 2a). Additional heavy labeling for GP2 was dispersed in spotty areas on the lateral cell surface (Fig. 2c), and may have corresponded to the punctate signals captured by confocal microscopy (Fig. 1c and d).

Expression of the Spi-B transcription factor in GP2-expressing cells

We investigated other important molecules expressed in the M cells of Peyer's patches. Spi-B is a transcription factor that is essential for M-cell differentiation (de Lau et al. 2012; Kanaya et al. 2012; Sato et al. 2013). Immunohistochemistry for Spi-B labeled a number of nuclei in the FAE of NALT (Fig. 3a). Multicolor fluorescent *in situ* hybridization (FISH) experiments showed that *Gp2*-expressing cells expressed *Tnfaip2* and *Spib* (Fig. 3 b-f). GP2-immunoreactive cells were labeled by antibodies against CCL9, which is an M-cell-expressing chemokine that is involved in the recruitment of dendritic cells to the dome region of Peyer's patches (Supplemental Fig. 2a and b) (Kanaya et al. 2012; Zhao et al. 2003). They also reacted with UEA-I lectin, a classical M-cell marker in the intestine (Supplemental Fig. 2c and d) (Clark et al. 1993). However, the specificity of UEA-I histochemistry was low because this method labeled not only a population of M cells but also other epithelial cells in the nasal cavity (Kimura et al. 2014). These molecular and morphological features indicated that $GP2^{+}Tnfaip2^{+}$ cells in the nasal cavity were typical M cells.

Uptake of luminal microbeads by $GP2^{+}Tnfaip2^{+}$ M cells

In order to verify whether M cells in NALT were functionally capable of taking up particles

from the lumen, we administered fluorescent microbeads into the nasal cavity 20 min before animals were sacrificed. Confocal microscopic observations showed that, even after such a short time course, some microbeads were incorporated and detected in M cells (Fig. 4). Immunoreactive GP2 at the apical plasma membrane was rarely detected after the microbeads of administration. Instead, GP2 was localized inside cells with a punctate pattern, and some of the dot-like immunoreactivities were colocalized with incorporated microbeads, indicating that GP2 at the apical cell surface was endocytosed with microbeads.

RANKL-RANK signaling controlled M-cell differentiation in NALT

RANKL has been shown to initiate the development of M cells in the intestinal epithelium (Knoop et al. 2009). Therefore, we herein assessed the expression of RANKL and its receptor, RANK, in the nasal cavity. Triple color immunofluorescent staining for RANKL, RANK, and Tnfaip2 revealed that many FAE cells reacted with the anti-RANK antibody, and stromal cells underneath the FAE were labeled with the anti-RANKL antibody (Fig. 5). RANK-expressing cells were closely localized to RANKL-immunoreactive stromal cells. Ordinary epithelia of the respiratory and olfactory areas did not express RANK. Most RANK-expressing cells in the FAE were also labeled with the anti-Tnfaip2 antibody, indicating that M cells expressed RANK in NALT. Therefore, we speculated that RANKL-RANK signaling was responsible for M-cell differentiation in the nasal cavity. In order to verify our hypothesis, we administered recombinant GST-RANKL protein to BALB/c mice intraperitoneally. The consecutive administration of RANKL for three days increased the number of $GP2^{+}$ and/or $Tnfaip2^{+}$ M cells in NALT (Fig. 6). Consistent with the limited localization of RANK-expressing cells to the

FAE in the nasal cavity, RANKL-induced M-cell formation was not detectable outside NALT. A quantitative image analysis revealed a significant increase in number in areas occupied by Tnfaip2-positive cells after the administration of RANKL (Fig. 6d).

RelB is a downstream transcription factor of RANKL-RANK signaling and is indispensable for intestinal M-cell differentiation (Kimura et al. 2015). Cells with RelB-positive nuclei also increased in number after the administration of RANKL, whereas control mice displayed RelB-positive nuclei in some FAE cells (Supplemental Fig. 3). Differential interference contrast (DIC) observations revealed a thickened epithelium in NALT in RANKL-administered mice (Fig. 7). The basal region of the thickened FAE was immunocytochemically characterized by the nuclear accumulation of Ki-67, the cell proliferation-associated antigen (Fig. 7). On the other hand, few Ki-67-immunoreactive cells were detected in the FAE of GST-administered mice, which were used as a control. The proportions of Ki-67 positive nuclei in the FAE were 31.8 ± 3.68% in the GST-RANKL-administered mice and 5.80 ± 4.19% in control mice, which was significantly different ($P < 0.001$, P-value calculated using the Student's t-test).

Discussion

In the present study, we demonstrated that $GP2^{+}Tnfaip2^{+}$ cells in the mouse nasal mucosa were equivalent to intestinal M cells, and RANKL-RANK signaling regulated the differentiation of M cells in NALT. Immunohistochemically, FAE in the NALT was shown to express RANK, and RANKL signals were detected in stromal cells underneath the FAE. Thus, the exogenous administration of RANKL markedly increased the number of M cells in NALT. The present study was the first to demonstrate RANKL-induced M-cell differentiation in the nasal cavity as well as to define the expression profile of molecules involved in M-cell maturation.

Research on the molecular mechanisms underlying M-cell differentiation has been recently advanced in the intestine. The administration of RANKL was previously shown to increase the number of M cells in the intestine (Knoop et al. 2009). In accordance with this finding, Peyer's patches from RANKL-null mice contained very few M cells in the FAE (Knoop et al. 2009). RelB is known to be activated by the RANKL-RANK interaction, resulting in its translocation from the cytoplasm to the nucleus (Kimura et al. 2015). Alymphoplasia mice, in which RelB failed to move into the nuclei, exhibited the deficient development of intestinal M cells (Kimura et al. 2015). The expression of Spi-B was previously shown to be dependent on the nuclear translocation of RelB. Spi-B-deficient mice lacked mature M cells in Peyer's patches and had a severely reduced capacity for the uptake of luminal antigens (Kanaya et al. 2012). In the present study, RelB was expressed in nuclei of NALT FAE cells, and RelB-expressing cells increased in number with the administration of RANKL. The expression of Spi-B mRNA in NALT was specific to M cells, as shown by triple-color FISH experiments, and the nuclear localization of the Spi-B protein was confirmed by immunohistochemistry.

Taken together, these results demonstrated that the expression profiles of RANKL-RANK, RelB, and Spi-B in NALT were almost identical to those in the M cells of Peyer's patches. These results further suggest that the regulatory machinery of M-cell differentiation is common between NALT and GALT.

The stem cells of intestinal M cells have been shown to reside and proliferate in the crypts (de Lau et al. 2012). In contrast, the proliferative site of nasal M cells remains unknown. Our RANKL administration also stimulated basal cell proliferation in the FAE of NALT. Immunohistochemistry for Spi-B showed that the nuclei of M cells were located in the basal portion of FAE; however, Ki-67 was scarcely detected in Spi-B-expressing M cells, indicating that proliferating cells were not differentiated M cells. Stem/progenitor cells of the pseudostratified epithelium of the airway are considered to be located in the basal layer and are capable of differentiating into other specialized cell types. Since RANKL is expressed by stromal cells underneath the FAE, RANKL may act on RANK-positive stem/progenitor cells and stimulate cell division in order to initiate the differentiation of M cells. RANK was expressed in Tnfaip2-positive differentiated M cells, suggesting that RANKL-RANK signaling was persistently required for the maturation and/or maintenance of M cells in NALT.

GP2 is a membrane–associated secretory protein that was originally identified in the zymogen granules of pancreatic acinar cells (Ronzio et al. 1978). This protein is also a well−known functional marker of intestinal M cells; GP2 appears in the later stage of M-cell differentiation, and its expression has been correlated with the uptake capacity of luminal microbeads (Hase et al. 2009a; Kimura et al. 2015). In the head region of mice, numerous GP2-expressing non-ciliated cells were found to be distributed in the epithelium covering the

paranasal sinuses, tear ducts, and conjunctiva (Kimura et al. 2014; our unpublished data). However, they did not express other M-cell markers, including UEA-I lectin, Tnfaip2, Spi-B, and CCL9. Histochemical studies suggested that GP2-expressing cells in the paranasal sinuses and conjunctiva were a lineage of goblet cells because they were more or less positive for Periodic Acid Schiff (PAS) staining (Kimura et al. 2014). GP2 may not be a specific marker for defining M cells in the nasal and ocular tissues of mice. In the present study, we demonstrated that $GP2^{+}Tnfaip2^{+}$ cells on the NALT FAE exhibited morphological features typical of M cells, shared the ability to uptake luminal microbeads, and expressed additional molecules specific to intestinal M cells. Furthermore, their differentiation was regulated by RANKL-RANK signaling. Therefore, we concluded that $GP2^{+}Tnfaip2^{+}$ cells in the nasal cavity corresponded to intestinal M cells.

Kim et al. (2011) recently reported that UEA-I^{+} M cells resided in the nasal respiratory epithelium. Although these UEA-I^{+} M cells were not associated with any lymphoid tissues, they were able to take up respiratory pathogens and initiate an antigen-specific immune response under an experimental condition. Our $GP2^{+}Tnfaip2^{+}$ M cells were also reactive with UEA-I lectin: however, their localization was restricted to the FAE of NALT. We did not detect any $GP2^{+}Tnfaip2^{+}$ cells or specific immunoreactivities for CCL9 and Spi-B in the respiratory area of the nasal mucosa, even after the administration of RANKL. A RANKL injection exclusively induced $GP2^{+}Tnfaip2^{+}$ M cells in the FAE, and not in the ordinary epithelium of the respiratory area. This result was consistent with the limited localization of its receptor RANK to the FAE. Therefore, UEA-I^{+} "M cells" outside NALT may differ from authentic M cells expressing GP2 and Tnfaip2, and their differentiation might be independent of RANKL-RANK

signals.

The present study demonstrated that RANKL-RANK signaling controlled M-cell differentiation in NALT as well as GALT. Downstream factors, RelB and Spi-B, may be involved in regulating the subsequent maturation process in both tissues. Accordingly, the fundamental molecules expressed in M cells were common to NALT and GALT. The results of this study showed that functional M cells were induced in the ciliated epithelium covering NALT as well as intestinal columnar epithelium, which have prompted us to continue our investigation, especially of the differentiation of M cells, in other mucosa-associated lymphoid tissues in the conjunctiva (CALT), tear duct (TALT), bronchus (BALT), and salivary gland duct (SALT/DALT) (Gebert and Pabst 1999; Nagatake et al. 2009; Nair and Schroeder 1986).

References

Asanuma H, Thompson AH, Iwasaki T, Sato Y, Inaba Y, Aizawa C, Kurata T, Tamura S (1997) Isolation and characterization of mouse nasal-associated lymphoid tissue. J Immunol Methods 202:123-131

Brandtzaeg Brandtzaeg P (1996) The B-cell development in tonsillar lymphoid follicles. Acta Otolaryngol Suppl 523:55-59

Carapelli A, Regoli M, Nicoletti C, Ermini L, Fonzi L, Bertelli E (2004) Rabbit tonsil-associated M-cells express cytokeratin 20 and take up particulate antigen. J Histochem Cytochem 52:1323-1332

Clark MA, Jepson MA, Simmons NL, Booth TA, Hirst BH (1993) Differential expression of lectin-binding sites defines mouse intestinal M-cells. J Histochem Cytochem 41:1679-1687

de Lau W, Kujala P, Schneeberger K, Middendorp S, Li VS, Barker N, Martens A, Hofhuis F, DeKoter RP, Peters PJ, Nieuwenhuis E, Clevers H (2012) Peyer's patch M cells derived from Lgr5(+) stem cells require SpiB and are induced by RankL in cultured "miniguts". Mol Cell Biol 32:3639-3647

Gebert A, Willfuhr B, Pabst R (1995) The rabbit M-cell marker vimentin is present in epithelial cells of the tonsil crypt. Acta Otolaryngol 115:697-700

Gebert A, Pabst R (1999) M cells at locations outside the gut. Semin Immunol 11:165-70.

Hase K, Kawano K, Nochi T, Pontes GS, Fukuda S, Ebisawa M, Kadokura K, Tobe T, Fujimura Y, Kawano S, Yabashi A, Waguri S, Nakato G, Kimura S, Murakami T, Iimura M, Hamura K, Fukuoka S, Lowe AW, Itoh K, Kiyono H, Ohno H (2009a) Uptake through glycoprotein 2 of FimH(+) bacteria by M cells initiates mucosal immune response. Nature 462:226-230

Hase K, Kimura S, Takatsu H, Ohmae M, Kawano S, Kitamura H, Ito M, Watarai H, Hazelett CC, Yeaman C, Ohno H (2009b) M-Sec promotes membrane nanotube formation by interacting with Ral and the exocyst complex. Nat Cell Biol 11:1427-32

Jeong KI, Uetsuka K, Nakayama H, Doi K (1999) Glycoconjugate expression in follicle-associated epithelium (FAE) covering the nasal-associated lymphoid tissue (NALT) in specific pathogen-free and conventional rats. Exp Anim 48:23-29

Jepson MA, Mason CM, Bennett MK, Simmons NL, Hirst BH (1992) Co-expression of vimentin and cytokeratins in M cells of rabbit intestinal lymphoid follicle-associated

epithelium. Histochem J 24:33-39

Kanaya T, Hase K, Takahashi D, Fukuda S, Hoshino K, Sasaki I, Hemmi H, Knoop KA, Kumar N, Sato M, Katsuno T, Yokosuka O, Toyooka K, Nakai K, Sakamoto A, Kitahara Y, Jinnohara T, McSorley SJ, Kaisho T, Williams IR, Ohno H (2012) The Ets transcription factor Spi-B is essential for the differentiation of intestinal microfold cells. Nat Immunol 13:729-736

Kim DY, Sato A, Fukuyama S, Sagara H, Nagatake T, Kong IG, Goda K, Nochi T, Kunisawa J, Sato S, Yokota Y, Lee CH, Kiyono H (2011) The airway antigen sampling system: respiratory M cells as an alternative gateway for inhaled antigens. J Immunol 186:4253-4262

Kimura S, Muto M, Hisamoto M, Zheng M, Iwanaga T (2014) A novel type of cells expressing GP2 in the respiratory epithelium of the paranasal sinuses in mice. Biomed Res 35:329-337

Kimura S, Yamakami-Kimura M, Obata Y, Hase K, Kitamura H, Ohno H, Iwanaga T (2015) Visualization of the entire differentiation process of murine M cells: suppression of their maturation in cecal patches. Mucosal Immunol 8:650-660

Knoop KA, Kumar N, Butler BR, Sakthivel SK, Taylor RT, Nochi T, Akiba H, Yagita H, Kiyono H, Williams IR (2009) RANKL is necessary and sufficient to initiate development of antigen-sampling M cells in the intestinal epithelium. J Immunol 183:5738-5747

Kuper CF, Hameleers DM, Bruijntjes JP, van der Ven I, Biewenga J, Sminia T (1990) Lymphoid and non-lymphoid cells in nasal-associated lymphoid tissue (NALT) in the rat. An immuno- and enzyme-histochemical study. Cell Tissue Res 259:371-377

Kuper CF, Koornstra PJ, Hameleers DM, Biewenga J, Spit BJ, Duijvestijn AM, van Breda Vriesman PJ, Sminia T (1992) The role of nasopharyngeal lymphoid tissue. Immunol Today 13:219-224

Lee JH, Kong SK, Wu ZS, Wu Q, Choe J, Cho HY, Ha SY, Kee SH, Kim YS (2010) Class II beta-tubulin is a novel marker for human tonsillar M cells and follicular dendritic cells. J Oral Pathol Med 39:533-539

Mabbott NA, Donaldson DS, Ohno H, Williams IR, Mahajan A (2013) Microfold (M) cells: important immunosurveillance posts in the intestinal epithelium. Mucosal immunol 6:666-677

Nagatake T, Fukuyama S, Kim DY, Goda K, Igarashi O, Sato S, Nochi T, Sagara H, Yokota Y,

Jetten AM, Kaisho T, Akira S, Mimuro H, Sasakawa C, Fukui Y, Fujihashi K, Akiyama T, Inoue J, Penninger JM, Kunisawa J, Kiyono H (2009) Id2-, RORgammat-, and LTbetaR-independent initiation of lymphoid organogenesis in ocular immunity. J Exp Med. 206:2351-64.

Nair PN, Schroeder HE (1986) Duct-associated lymphoid tissue (DALT) od minor salivary glands and mucosal immunity. Immunology 57: 171-80

Ronzio RA, Kronquist KE, Lewis DS, MacDonald RJ, Mohrlok SH, O'Donnell JJ, Jr. (1978) Glycoprotein synthesis in the adult rat pancreas. IV. Subcellular distribution of membrane glycoproteins. Biochim Biophys Acta 508:65-84

Sato S, Kaneto S, Shibata N, Takahashi Y, Okura H, Yuki Y, Kunisawa J, Kiyono H (2013) Transcription factor Spi-B-dependent and -independent pathways for the development of Peyer's patch M cells. Mucosal immunol 6:838-846

Stanley AC, Huntley JF, Jeffrey M, Buxton D (2001) Characterization of ovine nasal-associated lymphoid tissue and identification of M cells in the overlying follicle-associated epithelium. J Comp Pathol 125:262-270

Verbrugghe P, Kujala P, Waelput W, Peters PJ, Cuvelier CA (2008) Clusterin in human gut-associated lymphoid tissue, tonsils, and adenoids: localization to M cells and follicular dendritic cells. Histochem Cell Biol 129:311-320

Zhao X, Sato A, Dela Cruz CS, Linehan M, Luegering A, Kucharzik T, Shirakawa AK, Marquez G, Farber JM, Williams I, Iwasaki A (2003) CCL9 is secreted by the follicle-associated epithelium and recruits dome region Peyer's patch $CD11b^{+}$ dendritic cells. J Immunol.171:2797-803.

Figure captions

Fig. 1

Glycoprotein 2 (GP2) and Tnfaip2 double-positive cells in the follicle-associated epithelium (FAE) of mouse nasopharynx-associated lymphoid tissue (NALT).

(**a**) Hematoxylin and eosin staining of a frontal section of the mouse head. Lymphatic follicles (arrows) are located on both sides of the nasal airway. (**b**) A confocal microscope image of a double-stained section of NALT for GP2 (magenta) and Tnfaip2 (green). (**c** and **d**) High magnification images of GP2 and Tnfaip2 double-positive cells residing in the pseudostratified ciliated epithelium covering NALT. Three-color fluorescence images are shown with or without differential interference contrast (DIC) images (**c** and **d**, respectively). Arrows indicate dot-like GP2 immunoreactivities in the deeper region of the FAE. Bars: 100 μm (**b**), and 20 μm (**c** and **d**).

Fig. 2

Transmission electron micrographs of the NALT FAE immunostained for GP2.

(**a**) A GP2-immunoreactive M cell (M) lacks cilia at its apical surface and embraces a lymphoid cell (L). N: the nucleus of the M cell. (**b**) High magnification of another M cell displaying thick stubby microvilli on the free surface. Immunoreaction products were intensely precipitated along the apical cell surface. (**c**) A closer view of Figure 2a showing extracellular, heavy labeling for GP2 between an M cell (M) and lymphocyte (L). Bars: 2 μm (**a**), 1 μm (**b**), and 0.5 μm (**c**).

Fig. 3

Spi-B transcription factor was expressed in GP2 and Tnfaip2 double-positive cells.

(**a**) A confocal microscopy image of a section of NALT immunohistochemically stained for Spi-B. IHC: immunohistochemistry. (**b**) Three-color fluorescence *in situ* hybridization (FISH) image of the NALT FAE using oligonucleotide probes for *Tnfaip2* (magenta), *Spib* (cyan), and *Gp2* (green). (**c**-**f**) Enlarged views of the squared areas in **b**. Each of the indicated channels is shown separately. Bars: 20 μm (**a** and **b**) and 10 μm (**c**-**g**).

Fig. 4

Uptake of luminal latex beads by GP2 and Tnfaip2-double positive cells in the FAE of NALT.

Latex beads (magenta) were dropped into the nasal cavities of BALB/c mice, as described in the Methods section. Confocal images of NALT immunostained for Tnfaip2 (cyan) and GP2 (green) show two different fields (**a, b** and **d**, **e**). (**c** and **f**) Enlarged view of the squared areas in **a** and **d**, respectively. Signals for GP2 (green) and latex beads (magenta) were dispersed in the cytoplasm of GP2-immunoreactive cells. Arrows indicate the colocalization of GP2 signals and latex beads. Bars: 10 μm (**a**, **b**, **d** and **e**) and 5 μm (**c** and **f**).

Fig. 5

Triple immunostaining for Tnfaip2 (cyan), receptor activator of NF-κB (RANKL) (green), and its ligand RANKL (magenta).

Tnfaip2-labeled M cells express RANK and show an intimate relationship to RANKL-expressing cells underneath the FAE. Each of the indicated channels is shown

separately. Bars: 20 μm.

Fig. 6

Induction of M cells in NALT by the administration of RANKL.

(**a** and **b**) Confocal images of Tnfaip2 (green) and GP2 (magenta) in the NALT of glutathione S-transferase (GST) (**a**: as a control) or GST-RANKL-injected mice (**b**). (**c**) High magnification images of the FAE from a GST-RANKL-injected mouse. (**d**) A scatter plot showing the percentage of the area counting Tnfaip2-expressing cells in the FAE. Each dot represents the value of an individual FAE and horizontal bars indicate median values. The results are based on three mice. ***P<0.001: P-value was calculated by Student's t-test. Bars: 100 μm (**a** and **b**) and 40 μm (**c**).

Fig. 7

Stimulated cell proliferation in the FAE of NALT by the administration of RANKL.

An injection of GST-RANKL (**b**) increased the thickness of FAE more than a GST injection (**a**, control), as shown by DIC images. Conventional observations of the same areas showed an increased number of cells with Ki-67-labeled nuclei (**c**, **d**). Bars: 40 μm.

Supplemental Figures

Supplemental Fig. 1

Scanning electron micrograph of the luminal surface of NALT.

(a) M cells (arrows) are intermingled among ciliated cells. (b) High magnification of an M cell displaying thick stubby microvilli (arrows) and short microfolds (arrowheads). Bars: 10 μm (**a**) and 5 μm (**b**).

Supplemental Fig. 2

GP2-expressing cells in the NALT FAE expressed chemokine CCL9 and reacted with *Ulex europaeus* agglutinin I (UEA-I) lectin.

(**a** and **b**) A confocal microscope image of a double-stained section of NALT for CCL9 (green) and GP2 (magenta) with or without DIC images (**a** and **b**, respectively). (**c** and **d**) UEA-I lectin (green) labeled numerous epithelial cells on the FAE and ordinary respiratory epithelium. GP2-expressing cells (magenta) on the FAE occupied only a small population of UEA-I-labeled cells. Bars: 20 μm (**a** and **b**), 100 μm (**a**) and 50 μm (**b**).

Supplemental Fig. 3

The administration of RANKL increased the number of RelB-positive cells on the NALT FAE.

Confocal images of RelB (green) in the NALT of GST (**a** and **b**) or GST-RANKL-injected mice (**c** and **d**). (**b** and **d**) At a high magnification, the FAE from a GST-RANKL-injected mouse contained many RelB-positive nuclei in the basal layer (**d**). Bars: 100 μm (**a** and **c**) and 50 μm (**b** and **d**).

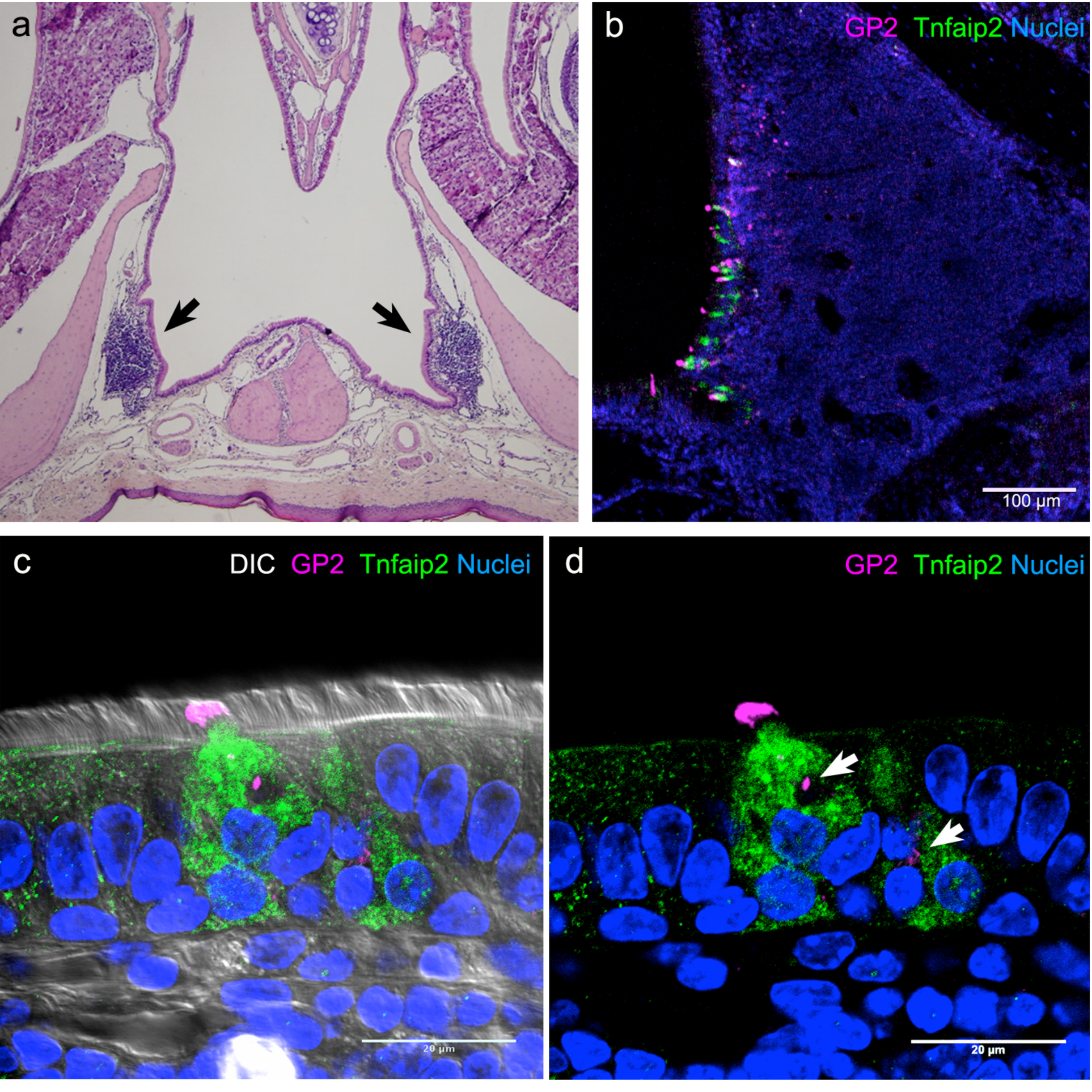
a
b
GP2 Tnfaip2 Nuclei
100 µm
c
DIC GP2 Tnfaip2 Nuclei
20 µm
d
GP2 Tnfaip2 Nuclei
20 µm

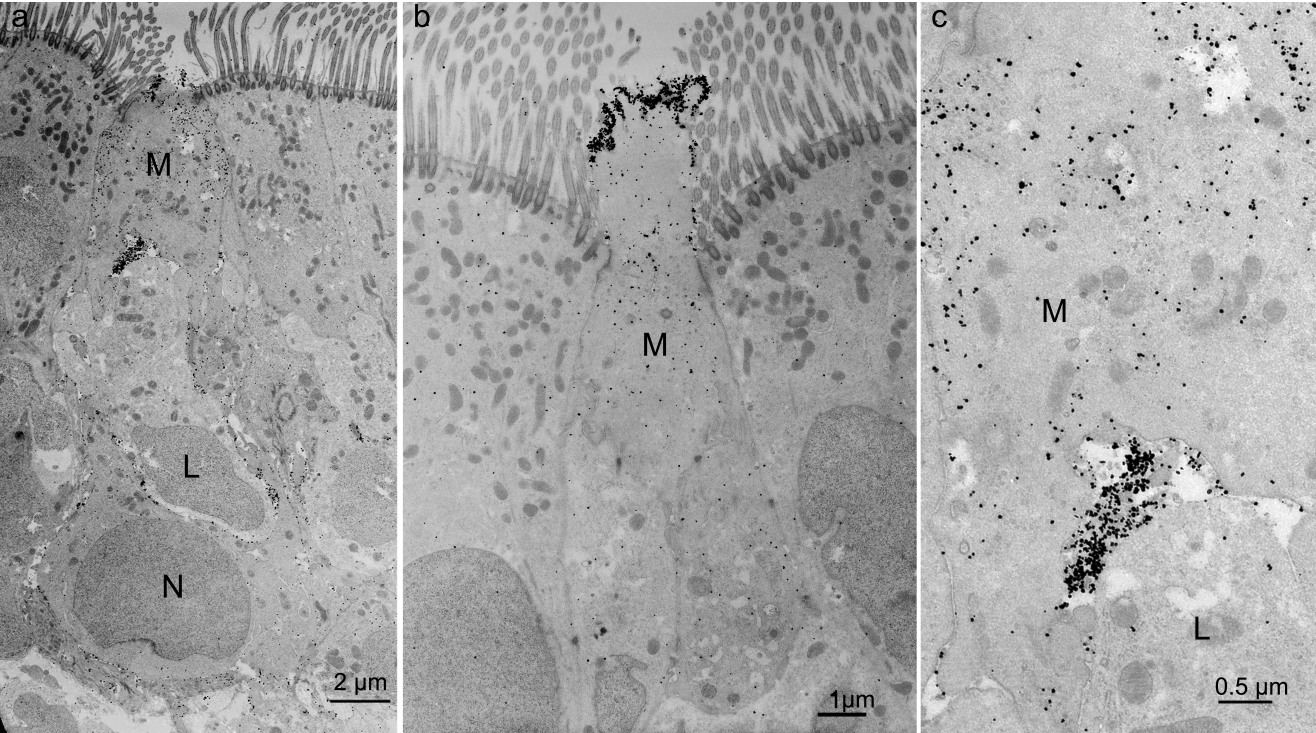
a
M
L
N
2 μm
b
M
1μm
c
M
L
0.5 μm

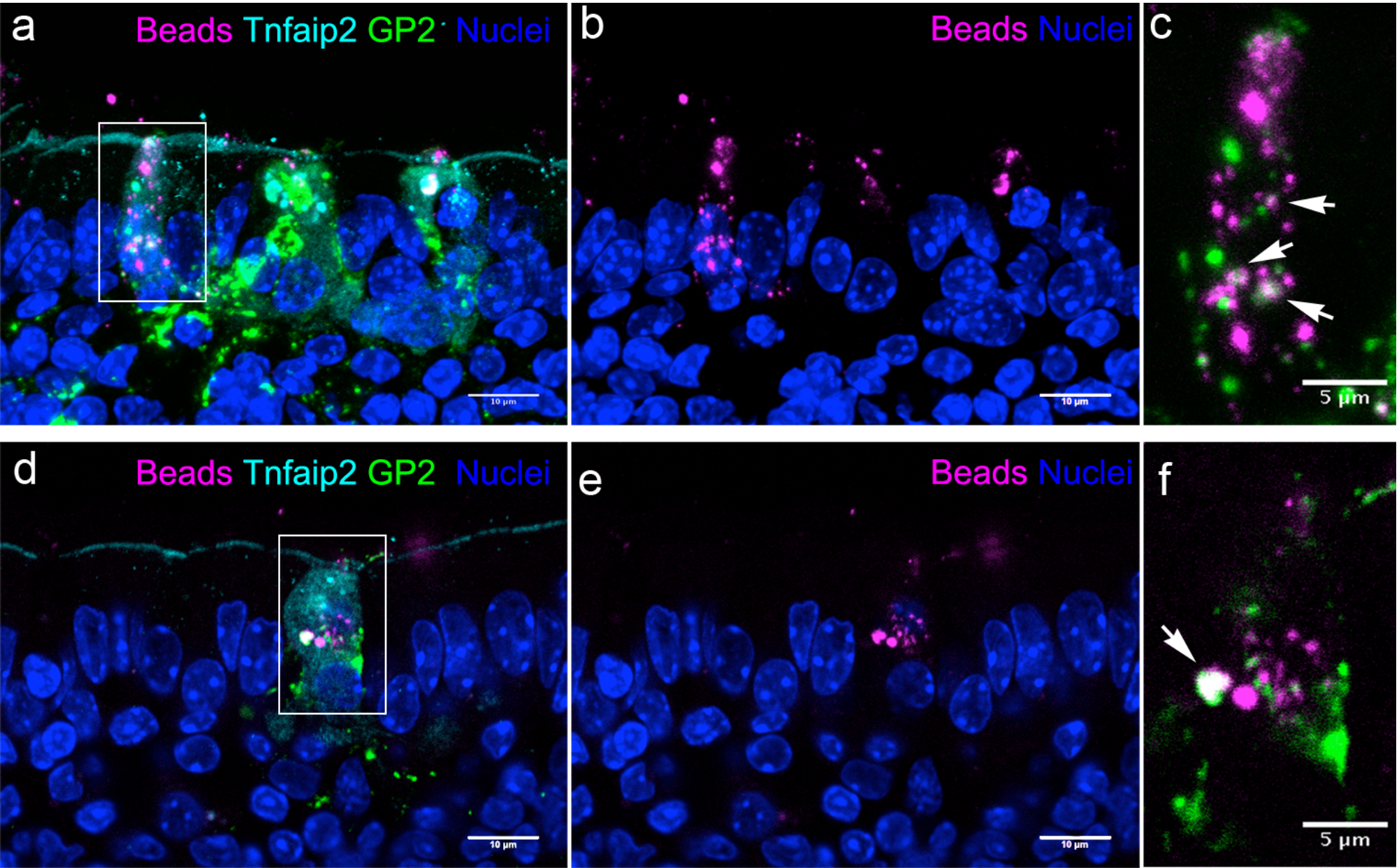
a
Beads Tnfaip2 GP2 Nuclei
10 µm
b
Beads Nuclei
10 µm
c
5 µm
d
Beads Tnfaip2 GP2 Nuclei
10 µm
e
Beads Nuclei
10 µm
f
5 µm

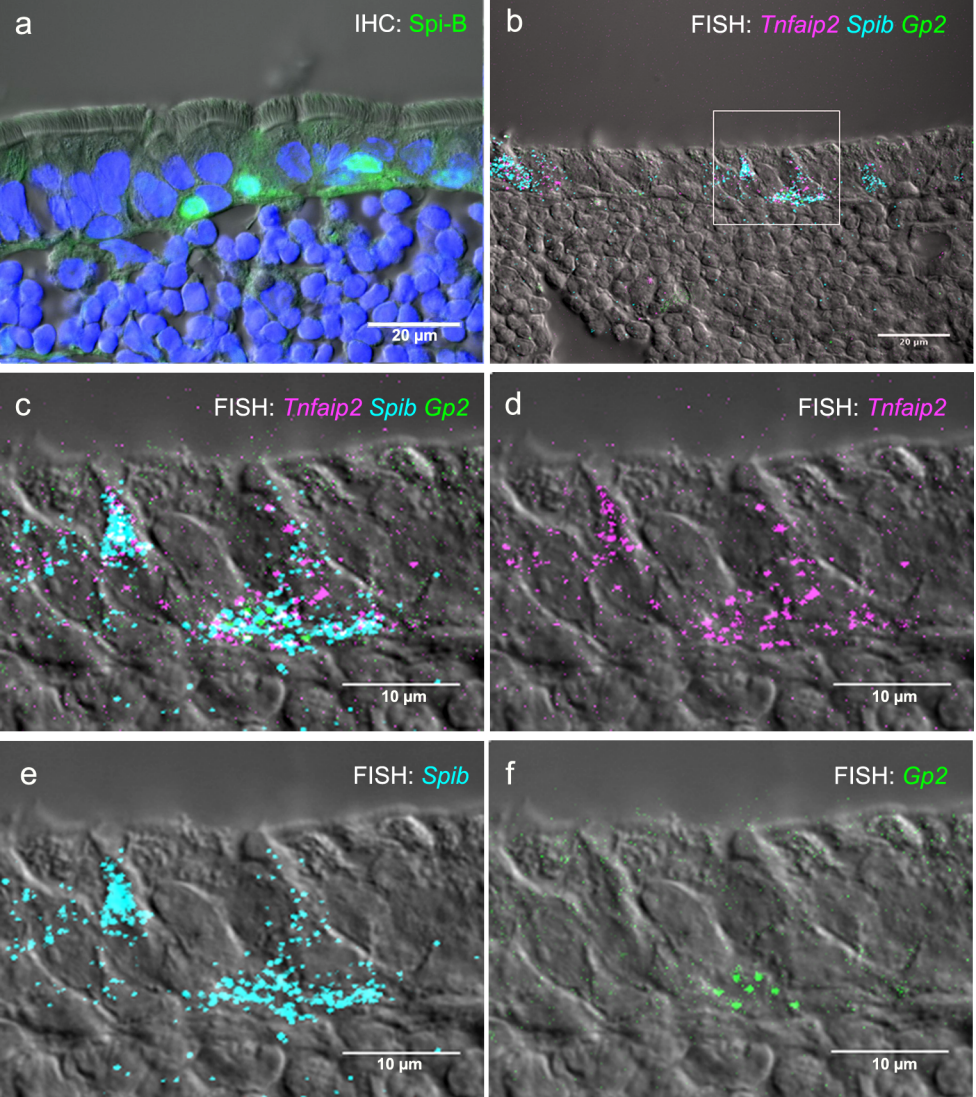
a
IHC: Spi-B
20 µm
b
FISH: Tnfaip2 Spib Gp2
20 µm
c
FISH: Tnfaip2 Spib Gp2
10 µm
d
FISH: Tnfaip2
10 µm
e
FISH: Spib
10 µm
f
FISH: Gp2
10 µm

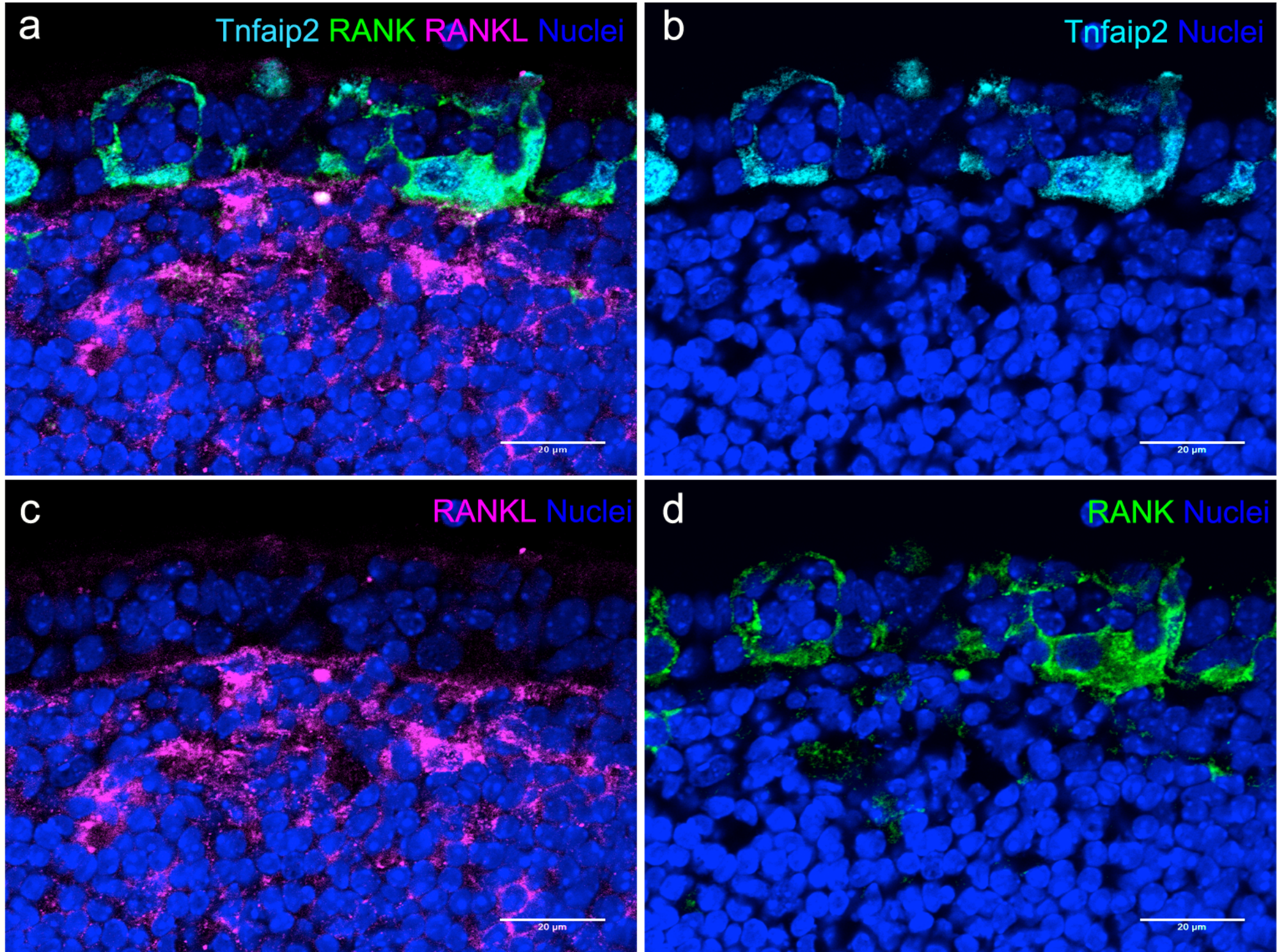
a
Tnfaip2 RANK RANKL Nuclei
20 µm
b
Tnfaip2 Nuclei
20 µm
c
RANKL Nuclei
20 µm
d
RANK Nuclei
20 µm

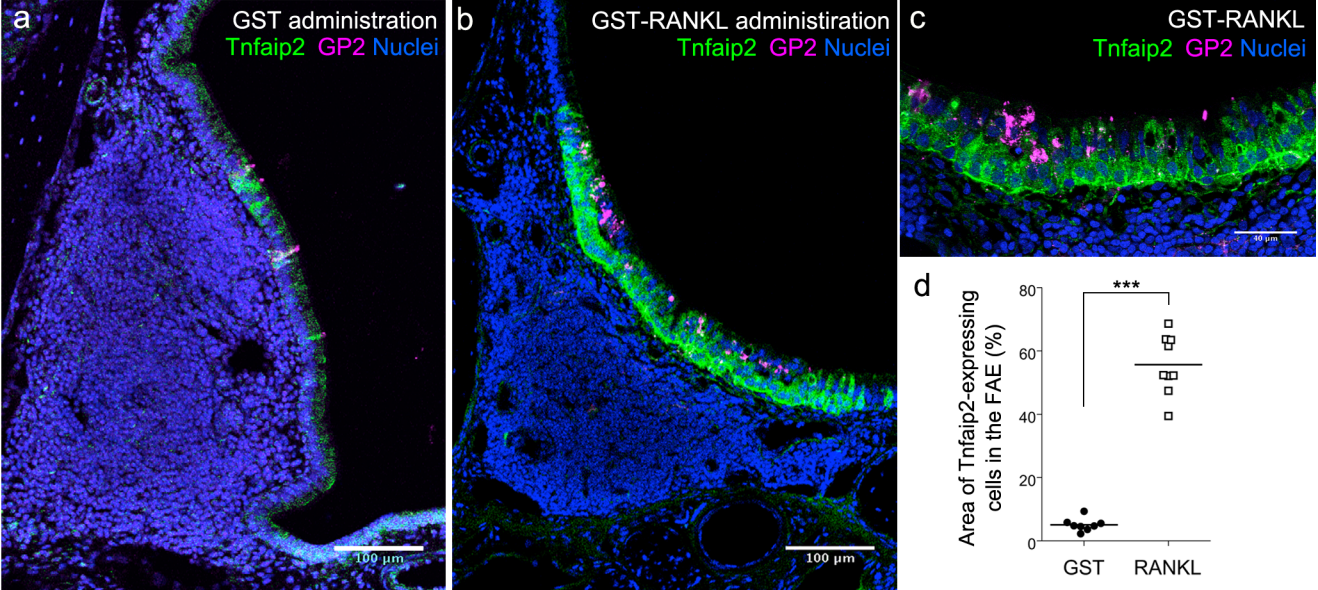
a
GST administration
Tnfaip2 GP2 Nuclei
100 μm
b
GST-RANKL administration
Tnfaip2 GP2 Nuclei
100 μm
c
GST-RANKL
Tnfaip2 GP2 Nuclei
40 μm
d
Area of Tnfaip2-expressing cells in the FAE (%)
***
80
60
40
20
0
GST
RANKL

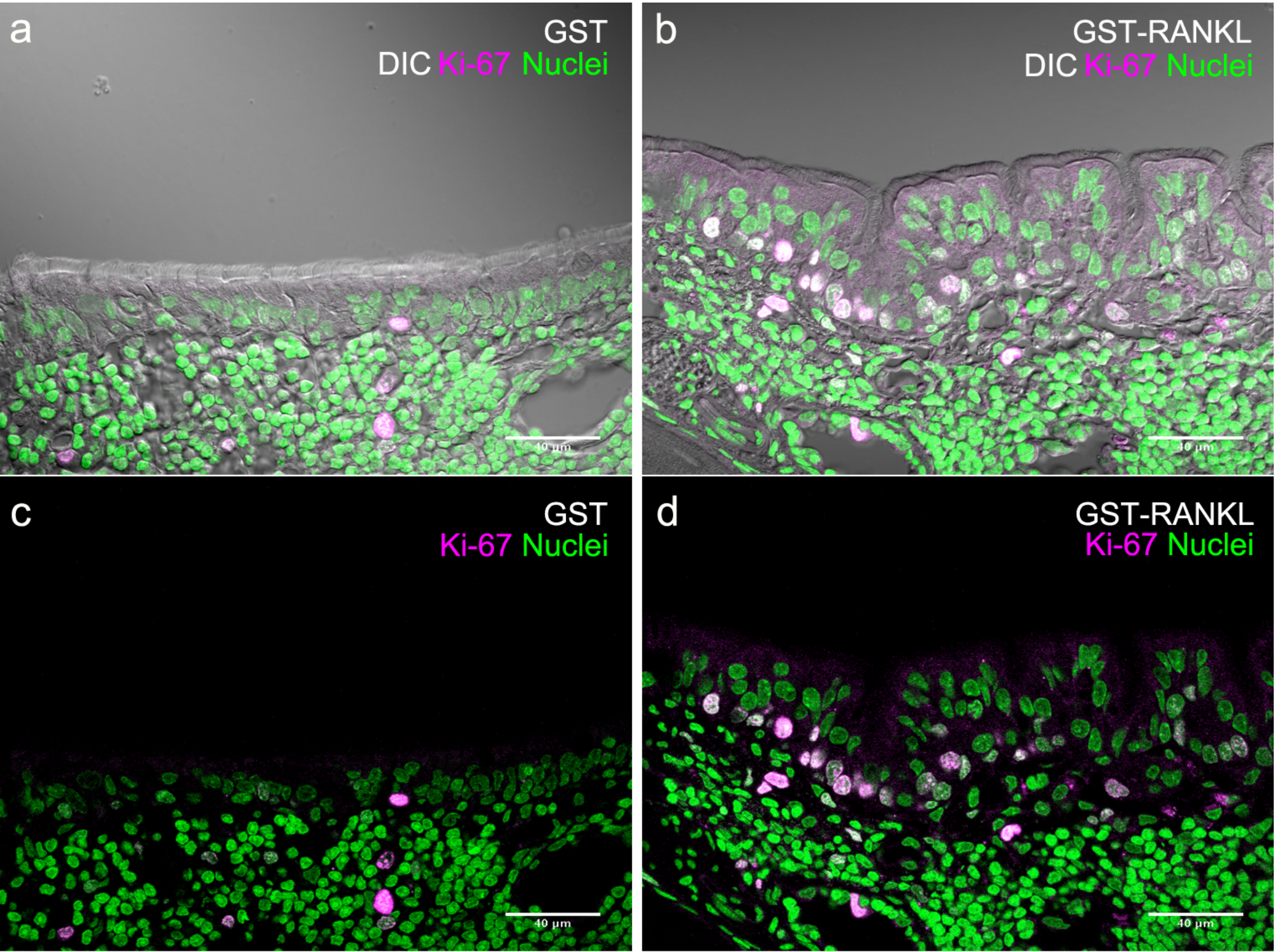
a
GST
DIC Ki-67 Nuclei
40 µm
b
GST-RANKL
DIC Ki-67 Nuclei
40 µm
c
GST
Ki-67 Nuclei
40 µm
d
GST-RANKL
Ki-67 Nuclei
40 µm

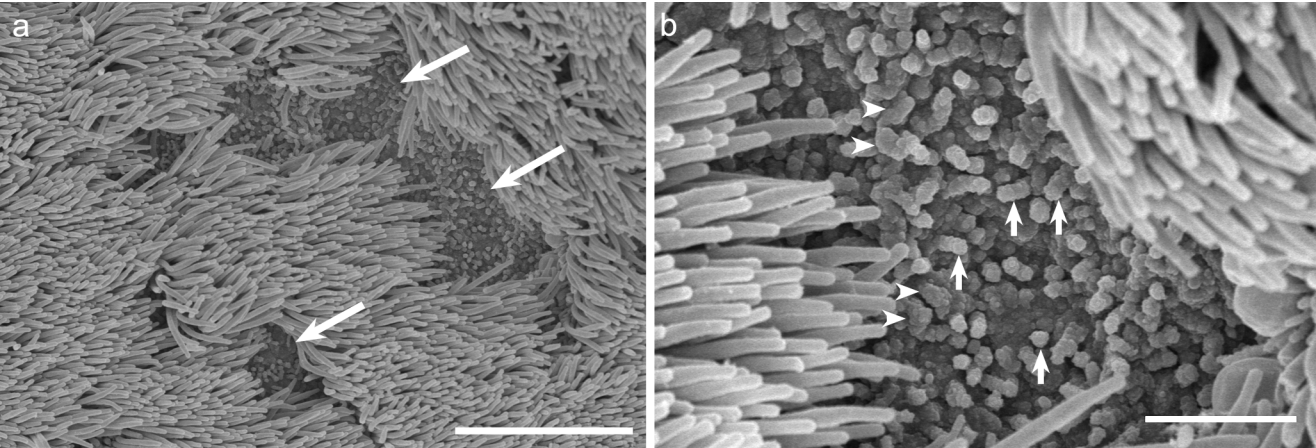
a
b

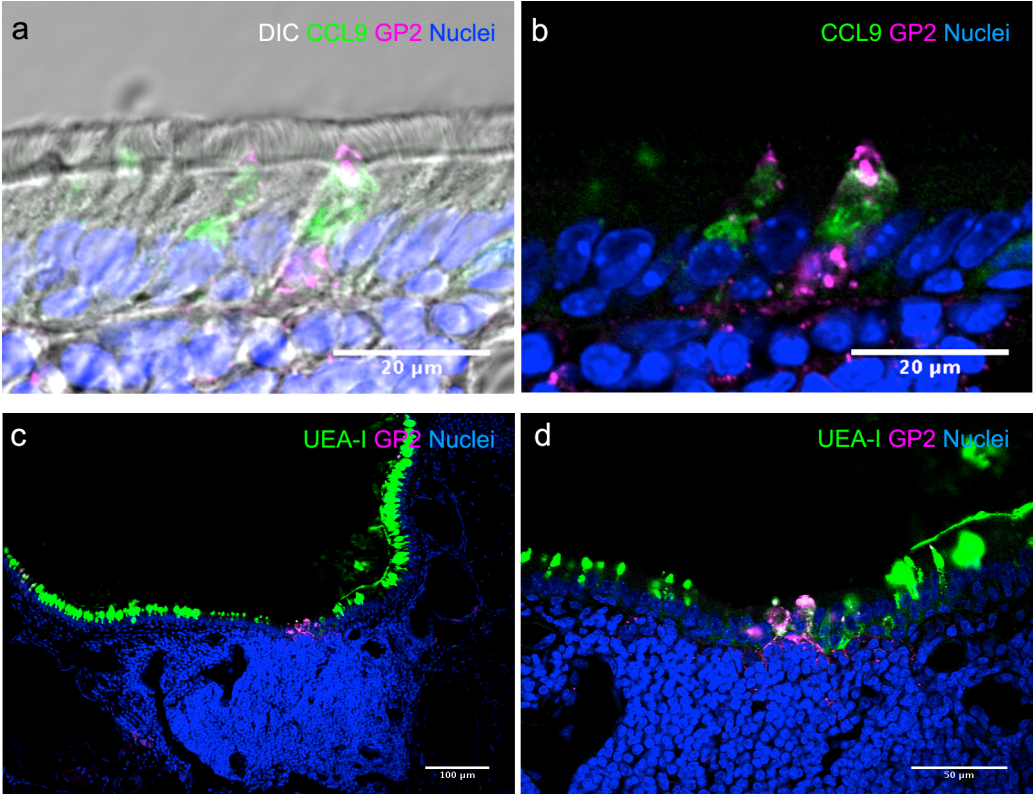
a
DIC CCL9 GP2 Nuclei
20 µm
b
CCL9 GP2 Nuclei
20 µm
c
UEA-I GP2 Nuclei
100 µm
d
UEA-I GP2 Nuclei
50 µm

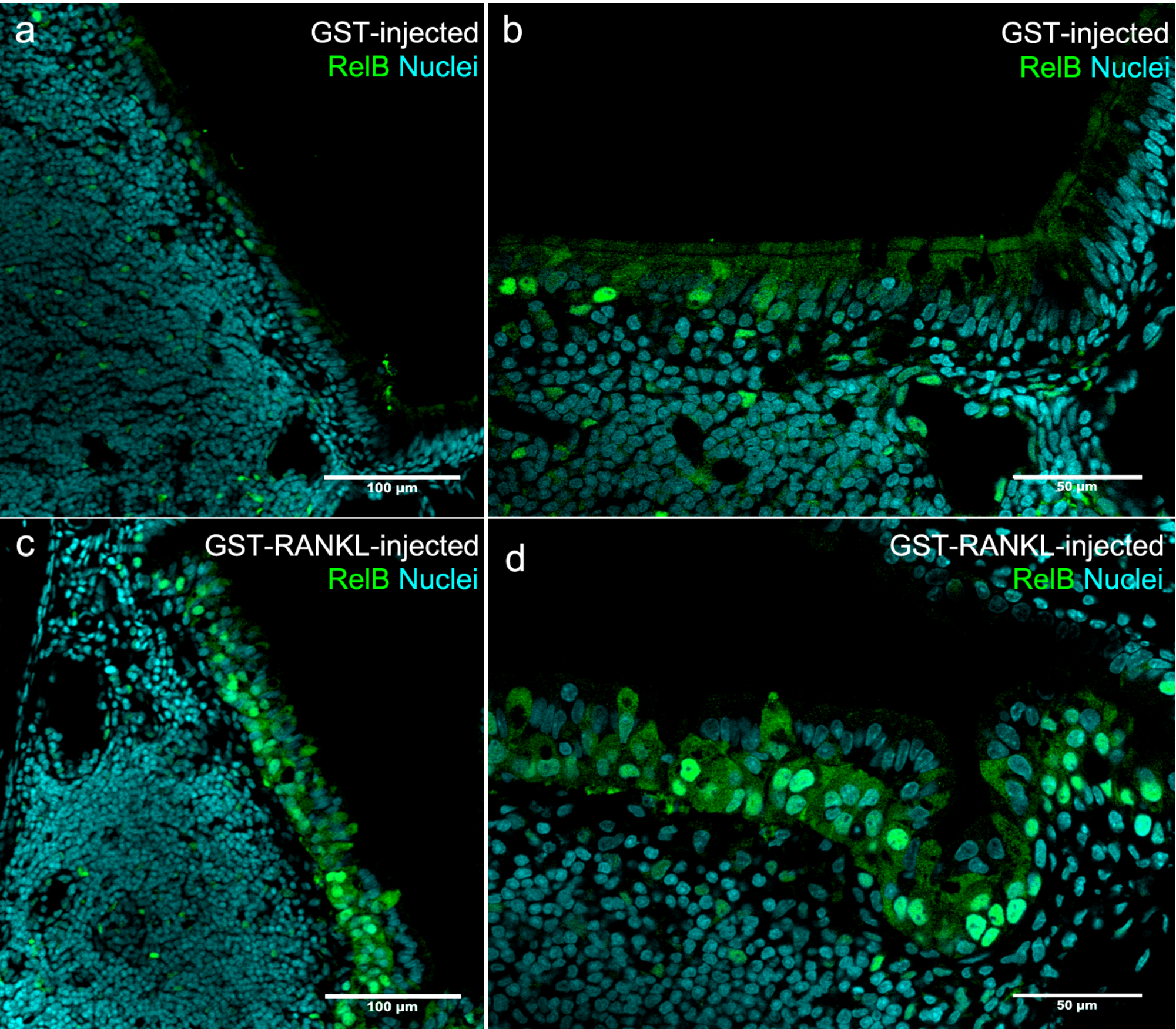
a
GST-injected
RelB Nuclei
100 µm
b
GST-injected
RelB Nuclei
50 µm
c
GST-RANKL-injected
RelB Nuclei
100 µm
d
GST-RANKL-injected
RelB Nuclei
50 µm